Original Article

www.jmss.mui.ac.ir

Three-dimensional Segmentation of Retinal Cysts from Spectral-domain Optical Coherence Tomography Images by the Use of Three-dimensional Curvelet Based K-SVD

Mahdad Esmaeili[1,2], Alireza Mehri Dehnavi[2], Hossein Rabbani[2], Fedra Hajizadeh[3]

[1]Department of Advanced Medical Technology, Isfahan University of Medical Sciences, Isfahan, [2]Medical Image and Signal Processing Research Center, Isfahan University of Medical Science, Isfahan [3]Noor Ophthalmology Research Center, Noor Eye Hospital, Tehran, Iran

Submission: 03-02-2016 Accepted: 04-05-2016

ABSTRACT

This paper presents a new three-dimensional curvelet transform based dictionary learning for automatic segmentation of intraretinal cysts, most relevant prognostic biomarker in neovascular age-related macular degeneration, from 3D spectral-domain optical coherence tomography (SD-OCT) images. In particular, we focus on the Spectralis SD-OCT (Heidelberg Engineering, Heidelberg, Germany) system, and show the applicability of our algorithm in the segmentation of these features. For this purpose, we use recursive Gaussian filter and approximate the corrupted pixels from its surrounding, then in order to enhance the cystoid dark space regions and future noise suppression we introduce a new scheme in dictionary learning and take curvelet transform of filtered image then denoise and modify each noisy coefficients matrix in each scale with predefined initial 3D sparse dictionary. Dark pixels between retinal pigment epithelium and nerve fiber layer that were extracted with graph theory are considered as cystoid spaces. The average dice coefficient for the segmentation of cystoid regions in whole 3D volume and with-in central 3 mm diameter on the MICCAI 2015 OPTIMA Cyst Segmentation Challenge dataset were found to be 0.65 and 0.77, respectively.

Key words: *Biomarkers, Cysts, Dictionary learning, Digital curvelet transform, Optical coherence tomography, Nerve fibers, Noise, Retinal pigment epithelium, Wet macular degeneration*

INTRODUCTION

Spectral-domain optical coherence tomography (SD-OCT) is a rapidly developing noninvasive cross-sectional imaging modality which allows to investigate the presence of choroidal neovascularization activity defined as the appearance of subretinal fluid, intraretinal cysts, intraretinal fluid, subretinal pigment epithelium (RPE) fluid, or a combination thereof to assist the diagnosis and management of neovascular age-related macular degeneration.[1] The intraretinal fluid spaces reduced retinal reflectivity than the surrounding tissues and can cause increased retinal thickness. Cyst regions can be manually segmented using SD-OCT,[2] but the manual segmentation of these regions from the large amount of imaging data produced in an SD-OCT volume may not be feasible and is time-consuming and extremely laborious. A number of segmentation algorithms have been proposed to identify fluid-filled regions.[3-5] However, these methods are not fully automatic and rely on manual initialization in each B-scan to segment the volume of cystoid regions. Furthermore, OCT images suffer from speckle noise which causes difficulty in the actual detection of retinal layers [Figure 1][6] and the shape of structural features such as drusens, macular holes, macular edema, nerve fiber atrophy, and cysts, that can be used as markers in clinical investigation and diagnostics of retinal diseases. Hence, before segmentation of this region in OCT images, the development of algorithmic approaches to provide noise suppression must be performed. In recent years, some approaches have been heavily investigated for speckle noise reduction, such as anisotropic diffusion-based methods,[7-9] wavelet–based methods,[10] dual-tree complex wavelet transformation,[11] curvelet transform,[12] contourlet transform,[13] sparsity-based denoising,[14,15] dictionary learning-based methods.[16,17]

Address for correspondence:
Prof. Alireza Mehri Dehnavi, Department of Advanced Medical Technology, Isfahan University of Medical Sciences, Isfahan, Iran.
E-mail: mehri@med.mui.ac.ir

How to cite this article: Mahdad Esmaeili M, Dehnavi AM, Rabbani H, Hajizadeh F. Three-dimensional Segmentation of Retinal Cysts from Spectral-domain Optical Coherence Tomography Images by the Use of Three-dimensional Curvelet Based K-SVD. J Med Sign Sence 2016;6:166-171.

Here, a novel speckle noise reduction algorithm is used,[18] which is optimized to reduce speckle in an OCT image while maintaining strong edge sharpness. For this purpose, we first apply recursive Gaussian filter to the noisy image and zero possible pixels are approximated from surrounding pixels then we introduce K-SVD dictionary learning in curvelet transform domain for speckle noise reduction of three-dimensional (3D) OCT images. As the noise more affected low scale of curvelet coefficients and to take advantage of this sparse multiscale directional transform, we introduce a new scheme in dictionary learning and take curvelet transform of noisy image then denoise and modify each noisy coefficients matrix in each scale with predefined initial 3D sparse dictionary. The 3D initial dictionary for every scale in each rotation is independently selected from thresholded coefficients in the same scale and rotation of logarithmic transformation of image and does not need any high-SNR scans (averaged versions of repeated scans) for dictionary learning. After denoising 3D OCT images pixels in image are adjusted and thresholded to segment possible fluid space candidate pixels. Then nerve fiber layer (NFL) and RPE layer are extracted in each B-scan by the use of graph theory.[19] Identification of these lines is used to define our retinal regions of interest (ROI) in each B-mode image. Finally, the possible false positives (FPs) are eliminated based on standard deviation and morphology of extracted candidate pixels.

The organization of this paper is as follows. Section 2 discusses the 3D curvelet based dictionary learning denoising algorithm, and section 3 shows an implementation of the algorithm for candidate cystoid space determination as well as our generalized method for removing missed extracted pixels, and results are presented in section 4. Finally, we conclude and give some perspectives for future work.

MATERIALS AND METHODS

Image Data

We implemented the proposed method on four 3D-OCT volumes obtained from Spectralis SD-OCT (Heidelberg Engineering, Heidelberg, Germany) system that each contained 49, 512 × 496 B-scans. The database containing retinal cysts together with manually labeled cystoid spaces were provided by the OPTIMA cyst segmentation challenge.

Optical Coherence Tomography Denoising

Although the direct analyzing of 3D data as a volume and also considering the 3D geometrical nature of the data is computationally expensive, but it has been shown that 3D analysis of 3D data outperforms 2D slice-by-slice analyzing.[20] 3D curvelet elements are plate-like shapes of $2^{-j/2}$ in two directions and width about 2^{-j} in the orthonormal direction which are smooth within the plate and oscillates along the normal direction of the plate. The parabolic scaling, direction, tightness, and sparse representation properties of this 3D multiscale transform, provide new opportunities to analyze large data sets in medical image processing. In this paper, we used a new implementation of the 3D fast curvelet transform (3DFCT)[21,22] that has a reduced redundancy factor than the wrapping-based implementation as proposed in CurveLab Toolbox[23,24] with the strong directional selectivity property at the finest scale.

For this purpose and taking curvelet coefficients:

1. Cartesian coronization is performed that decomposes the object into dyadic coronae based on concentric cubes. Each corona is subdivided into trapezoidal regions conforming the usual parabolic scaling as shown in Figure 2
2. The 3D coefficients are obtained by applying an inverse 3D FFT to each wrapped wedge as shown in Figure 1, that appropriately fits into a 3D rectangular parallelepipeds of dimensions ~ (2j, 2j/2, 2j/2) centered at the origin.

Since the curvelet coefficients have a sparse distribution, we have only a few large coefficients that show the main structure of image and the remained coefficients tend to zero.[23] This transform maps signals and noise into different

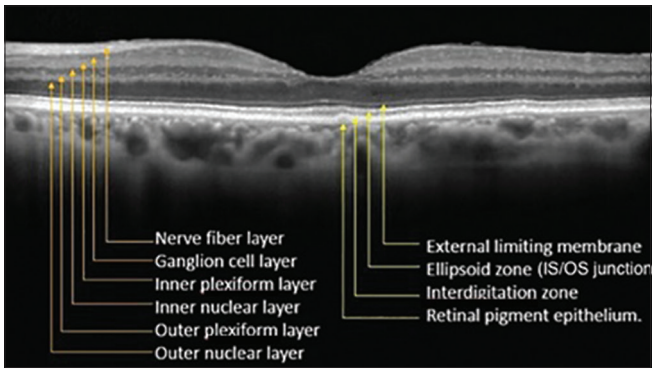

Figure 1: A cross-sectional, of a normal human retina with the layers identified

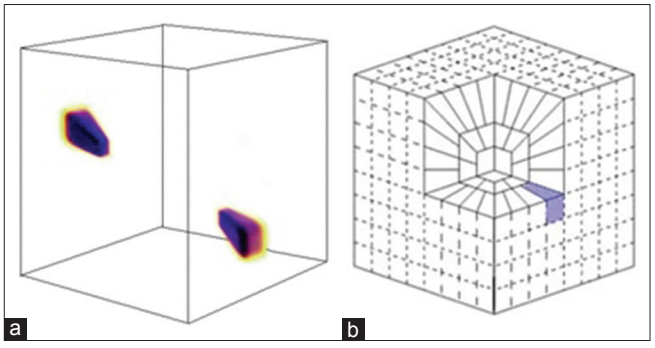

Figure 2: 3D rendering of curvelet atom in frequency (a), and discrete frequency tiling (b), the shaded area separates three-dimensional wedge

areas, and signal's energy is concentrated in a limited number of coefficients in curvelet domain.

OCT denoising can improve the image quality for the accurate analysis of image information, such as intra-retinal layers and boundaries of pathology that the results of accurate detection of these features are fully dependent on image enhancement through image denoising.[25,26] For this purpose in our selected dataset, all zero value corrupted pixels are determined from $5 \times 5 \times 5$ surrounding pixels based on recursive Gaussian filter.[27] After removing zero pixels, we used a novel speckle noise reduction algorithm that was previously implemented on 3D, SD-OCT, Bioptigen imaging systems.[18] Our curvelet-based approach consists of first transforming the noisy image using the 3DFCT, and taking curvelet coefficients, then in curvelet domain for each scale and rotation, the coefficient matrix is independently denoised based on K-SVD dictionary learning. A fundamental consideration in employing the KSVD dictionary learning is the selection of the start dictionary D. While some popular class of sparsity-based denoising algorithms exploits the information of the noisy image itself to define the dictionary,[14] however, the high-level of noise in the SDOCT images negatively contend with the learning process, degrades the quality of the trained dictionary. An alternative (ideal) approach is to learn the dictionary from the noiseless with high SNR image. Since in practice, such an ideal image is not available, so we select the initial dictionary from thresholded curvelet coefficients in same scale and rotation of logarithmic transformation of the noisy image [Eq. 1].

The hard threshold $T_{j,l}$ is applied to each curvelet coefficients such that:

$$C_{(j,l,p)} = \begin{cases} C_{(j,l,p)} & if \quad C_{(j,l,p)} \geq T_{j,l} \\ 0 & \text{else} \end{cases} \tag{1}$$

The threshold $T_{j,l}$ is selected based on so-called k-sigma method,[28] in which $T_{j,l} = k \times \sigma 1 \times \sigma 2$, where k is an adjustable parameter, $\sigma 1$ is the standard deviation of noise from a background region in the image data, and $\sigma 2$ is the standard deviation of noise in the curvelet domain at a specific scale j and orientation l.[28]

After finding the appropriate 3D initial dictionary, D, for each scale and orientation, the noisy curvelet coefficient matrixes of the noisy image in same scale and rotation are despeckled based on K-SVD dictionary learning.[19]

Since the curvelet transform is successful in dealing with edge discontinuities, it is a good candidate for edge enhancement. Hence, to enhance the contrast of intra-retinal layer boundaries, denoised curvelet coefficients, before taking 3D inverse discrete curvelet transform (3D-IDCUT), can be modified to enhance edges in an image.[29,30] A function must be defined which modifies the values of the curvelet coefficients by $k_c(C_{j,l,p})$ as follows:

$$k_c(x) = \begin{cases} 2x & if\ (x) < N \\ \left|\frac{x}{N}\right|^{0.3} x & if\ N \leq (x) < 3N \\ \left|\frac{M}{x}\right|^{0.5} x & if\ 3N \leq (x) \end{cases} \tag{2}$$

In Eq. 2 $N = 0.2\ M$, here M is the maximum curvelet coefficient of the relative band. Then we reconstruct the enhanced image from the denoised and modified curvelet coefficients by applying IDCUT. The outline of the whole denoising process is shown in Figure 3.

Candidate Cystoid Space Determination

In this section, we present a new candidate detection algorithm to separate the dark spaces from the rest of the image. During this process, each pixel $f(i, j, k)$ in despeckled image is adjusted as follows:

$$g(i,j,k) = f(i,j,k) + 0.5\bar{f}_W - \frac{80(Max(f_W))}{Min(f_W)+1} \tag{3}$$

where $\bar{f}w$, Max (fw) and Min (fw) are the mean, maximum and minimum intensity value of the image within a window W of size $3 \times 3 \times 3$, respectively. The dark cystoid spaces in adjusted image is trending to zero and is extracted by applying simple threshold ($t = 5$).

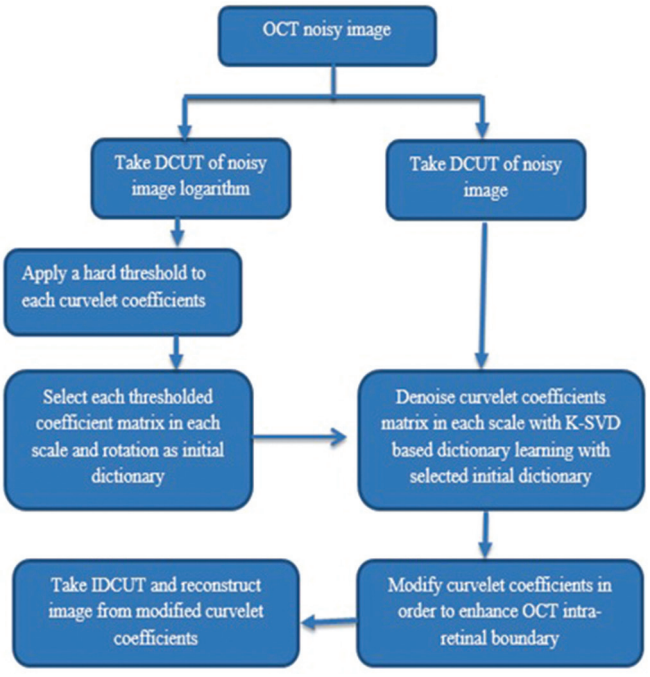

Figure 3: The outline of the proposed method for despeckling

Removing Miss Extracted Pixels

To improve the specificity, we reject FP pixels by extracting NFL and RPE layer in each B-scan by the use of graph theory.[31] We use these extracted lines to define the upper and lower bounds as retinal ROI in which we segment the cystoid fluid. Then we define and calculate the F ratio[32] and remove every connected component in ROI that has $F > 4$. This selection removes each connected component that has line shape structure belonging to dark regions between outer plexiform layer and outer nuclear layer. Figure 4 depicts the evaluation of F.

$$F = \frac{\max(m_i, m_j)}{\min(M_i, M_j)} \quad (4)$$

Where, M_i = max (width of a connected component in direction i) and M_j = max (width of a connected component in direction j) with m_i = max (i) – min (i), m_j = max (j) – min (j).

The distribution of pixel intensity in cystoid spaces are also uniform[4] so final cystoid volumes are extracted by rejecting regions with a standard deviation greater than an empirically determined value of 30. Figure 5 shows the results of this algorithm after removing miss extracted connected pixels that have $F > 4$ and regions with a standard deviation >30.

EXPERIMENTAL RESULTS

This study has focused on OCT images obtained from Spectralis SD-OCT (Heidelberg Engineering, Heidelberg, Germany) system provided by the OPTIMA laboratory for the cyst segmentation challenge hosted at MICCAI 2015. To evaluate the performance of this automated method, the method was applied on four 3D-OCT images each contain 49 B-scans, and the dice coefficients[33] of the segmented cystoid regions entire 3D volume, were compared against the two manually labeled grader. Figure 6 shows the results of our proposed algorithm.

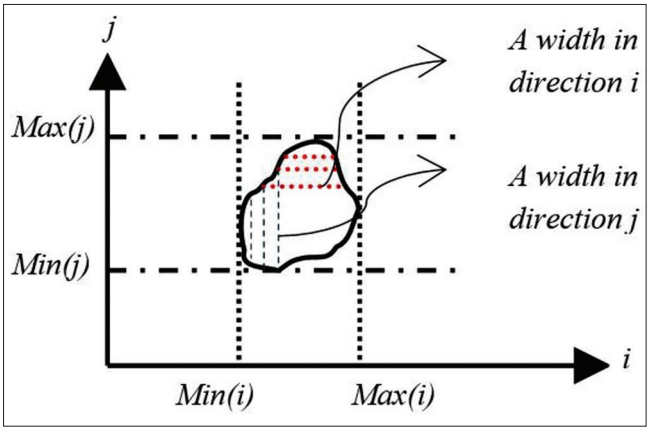

Figure 4: The evaluation F

The dice coefficient for each of the evaluated volumes and also the dice coefficient within central 3 mm diameter obtained for each volume are summarized in Table 1. We also computed the dice coefficients between the automated method and the intersection of the two readers for comparison.

DISCUSSION

This paper presented a new method for segmentation and quantification of the total volume occupied by intraretinal cystoid fluid from 3D OCT image. We tested our algorithm on four 3D Spectralis SD-OCT (Heidelberg Engineering, Heidelberg, Germany) images, each containing 49 B-scans. In this paper, we use the graph theory for extraction of NFL and RPE, the upper and lower bounds as retinal ROI, to increase the accuracy of detected bounds. A limitation of our work is that in the presence of epiretinal membrane, a fine piece of scar tissue that grows on the surface of the retina, some FPs are extracted that should be distinguish from intraretinal cysts. However, the proposed method revealed promising results, but further validation studies with larger samples are needed. The performance of the proposed method will be investigated on OCT images obtained by other scanners such as Topcon and Cirrus in future steps.

CONCLUSION

This paper presented a new algorithm to detect and segment the retinal cysts in an SDOCT volume. The calculation of F-ratio that uses the shape information of detected candidate regions removes each connected component that has line shape structure and will increase the accuracy of our proposed method. Although the proposed method can accurately detect the obvious cysts, it is not sensitive to the very small cysts, and the small cystoid regions that may be connected to the dark regions between outer plexiform layer and outer nuclear layer may not be detected accurately. Other possibilities can be studied to improve the proposed

Table 1: Evaluation of proposed method on against the two manually labeled grader

Evaluation using	Grader 1	Grader 2	intersection of Graders 1 and 2
Dice coefficient (s)			
Spectralis-1	0.7140	0.6817	0.7181
Spectralis-2	0.4549	0.4581	0.4501
Spectralis-3	0.6954	0.6501	0.6846
Spectralis-4	0.7115	0.7255	0.7307
Dice coefficient within central 3 mm diameter			
Spectralis-1	0.8173	0.7792	0.7918
Spectralis-2	0.7775	0.7769	0.7493
Spectralis-3	0.7563	0.7823	0.7652
Spectralis-4	0.7528	0.7732	0.7710

Figure 5: Results of this algorithm after removing miss extracted connected pixels, (a) original image (b) extracted candidate pixels (c) extracted cystoid regions after removing false positives

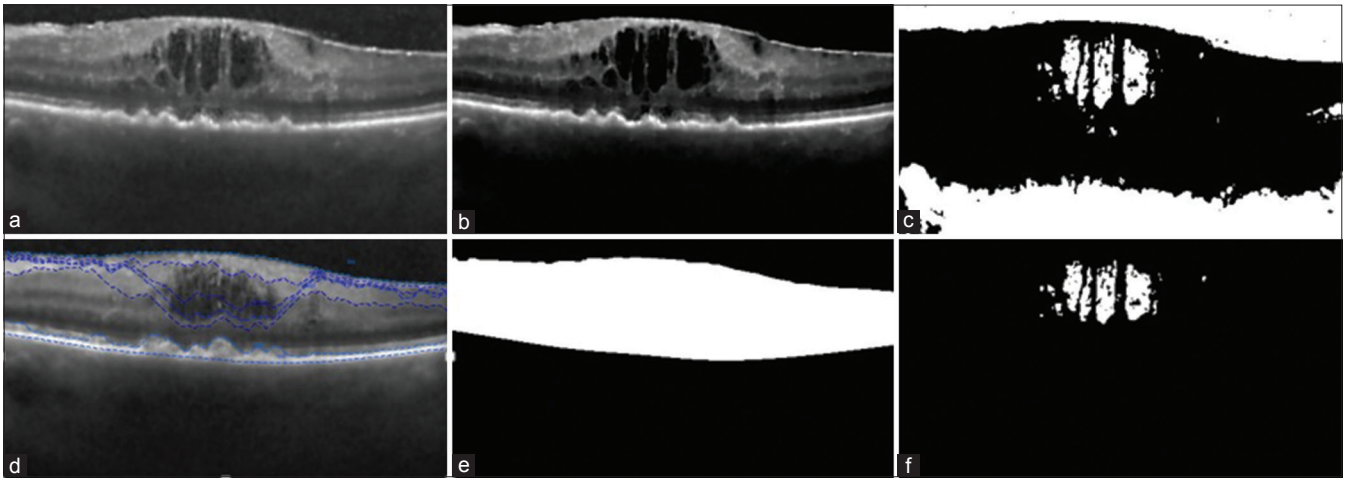

Figure 6: Results of our proposed method. (a) Despeckled image, (b) adjusted image (c) candidate cystoid pixels (d) detected internal limiting membrane and retinal pigment epithelium and other layers with graph theory (e) extracted regions of interest (f) segmented cystoid pixels

algorithm by detecting vessel shades to reduce the number of Fps.

Financial Support and Sponsorship

Nil.

Conflicts of Interest

There are no conflicts of interest.

REFERENCES

1. Hee MR, Puliafito CA, Wong C, Duker JS, Reichel E, Rutledge B, *et al.* Quantitative assessment of macular edema with optical coherence tomography. Arch Ophthalmol 1995;113:1019-29.
2. de Sisternes, Simon N, Tibshirani R, Leng T, Rubin DL, Quantitative SD-OCT imaging biomarkers as indicators of age-related macular degeneration progression predicting AMD progression using SD-OCT features. Invest Ophthalmol Vis Sci 2014;55:7093-103.
3. RoyChowdhuryS, KoozekananiD, RadwanS, Parhi k. Automated detection and location analysis of diabetic cysts in retinal OCT images: An iterative filtering approach. Invest Ophthalmol Vis Sci 2013;54:4901.
4. Wilkins GR, Houghton OM, Oldenburg AL. Automated segmentation of intraretinal cystoid fluid in optical coherence tomography. IEEE Trans Biomed Eng 2012;59:1109-14.
5. Zhang L, Zhu W, Shi F, Chen H, Chen X. Automated Segmentation of Intraretinal Cystoid Macular Edema for Retinal 3D OCT Images with Macular Hole. Biomedical Imaging (ISBI), 2015 IEEE 12th International Symposium on: IEEE; 2015. p. 1494-7.
6. Lee JG, Rosen RB. Learning to read retinal OCT. Ophthalmology Management 2015;19:44-6.
7. Aja S, Alberola C, Ruiz J. Fuzzy anisotropic diffusion for speckle filtering. IEEE Int Conf Acoust Speech Signal Process 2001;2:1261-4.
8. Puvanathasan P, Bizheva K. Interval type-II fuzzy anisotropic diffusion algorithm for speckle noise reduction in optical coherence tomography images. Opt Express 2009;17:733-46.
9. Yu Y, Acton ST. Speckle reducing anisotropic diffusion. IEEE Trans Image Process 2002;11:1260-70.
10. Luisier F, Blu T, Unser M. A new SURE approach to image denoising: Interscale orthonormal wavelet thresholding. IEEE Trans Image Process 2007;16:593-606.
11. Chitchian S, Fiddy MA, Fried NM. Denoising during optical coherence tomography of the prostate nerves via wavelet shrinkage using dual-tree complex wavelet transform. J Biomed Opt 2009;14:014031.
12. Jian Z, Yu Z, Yu L, Rao B, Chen Z, Tromberg BJ. Speckle attenuation in optical coherence tomography by curvelet shrinkage. Opt Lett 2009;34:1516-8.

13. Guo Q, Dong F, Sun S, Lei B, Gao BZ. Image denoising algorithm based on contourlet transform for optical coherence tomography heart tube image. IET Image Process 2013;7:442-50.
14. Elad M, Aharon M. Image denoising via sparse and redundant representations over learned dictionaries. IEEE Trans Image Process 2006;15:3736-45.
15. Fang L, Li S, Nie Q, Izatt JA, Toth CA, Farsiu S. Sparsity based denoising of spectral domain optical coherence tomography images. Biomed Opt Express 2012;3:927-42.
16. Fang L, Li S, McNabb RP, Nie Q, Kuo AN, Toth CA, *et al.* Fast acquisition and reconstruction of optical coherence tomography images via sparse representation. IEEE Trans Med Imaging 2013;32:2034-49.
17. Kafieh R, Rabbani H, Selesnick I. Three dimensional data-driven multi scale atomic representation of optical coherence tomography. IEEE Trans Med Imaging 2015;34:1042-62.
18. EsmaeiliM, DehnaviAM, RabbaniH, Hajizadeh F.3D Curvelet BasedDictionary Learning for Speckle Noise Reduction of Optical CoherenceTomography. 2015.
19. Aharon M, Elad M, Bruckstein A. The K-SVD: An algorithm for designing overcomplete dictionaries for sparse representation. IEEE Trans Signal Process 2006;54:4311-22.
20. Rabbani H, Sonka M, Abramoff MD. Optical coherence tomography noise reduction using anisotropic local bivariate gaussian mixture prior in 3D complex wavelet domain. Int J Biomed Imaging 2013;2013:417491.
21. Woiselle A, Starck JL, Fadili J. 3-D data denoising and inpainting with the low-redundancy fast curvelet transform. J Math Imaging Vis 2011;39:121-39.
22. Woiselle A, Starck JL, Fadili J. 3D curvelet transforms and astronomical data restoration. Appl Comput Harmon Anal 2010;28:171-88.
23. Candes E, DemanetL, DonohoD, Ying L. Fast discrete curvelet transforms. Multiscale Model Simul 2006;5:861-99.
24. Ying L, Demanet L, Candes E. 3D discrete curvelet transform. Appl Comput Math 2005;50:351-61.
25. Bonesi M, Proskurin S, Meglinski I. Imaging of subcutaneous blood vessels and flow velocity profiles by optical coherence tomography. Laser Phys 2010;20:891-9.
26. Kajic V, Povazay B, Hermann B, Hofer B, Marshall D, Rosin PL, *et al.* Robust segmentation of intraretinal layers in the normal human fovea using a novel statistical model based on texture and shape analysis. Opt Express 2010;18:14730-44.
27. Roomi SM, Lakshmi I, Kumar VA. A recursive gaussian weighted filter for impulse noise removal. GVIP J 2006;6:33-7.
28. Starck JL, Candès EJ, Donoho DL. The curvelet transform for image denoising. IEEE Trans Image Process 2002;11:670-84.
29. Esmaeili M, Rabbani H, Dehnavi AM. Automatic optic disk boundary extraction by the use of curvelet transform and deformable variational level set model. Pattern Recognit 2012;45:2832-42.
30. Esmaeili M, Rabbani H, Dehnavi AM, Dehghani A. Extraction of Retinal Blood Vessels by Curvelet Transform. 16th IEEE International Conference on Image Processing (ICIP); 2009. p. 3353-6.
31. Chiu SJ, Li XT, Nicholas P, Toth CA, Izatt JA, Farsiu S. Automatic segmentation of seven retinal layers in SDOCT images congruent with expert manual segmentation. Opt Express 2010;18:19413-28.
32. Esmaeili M, Rabbani H, Dehnavi AM, Dehghani A. A New Curvelet Transform Based Method for Extraction of Red Lesions in Digital Color Retinal Images. Image Processing (ICIP), 2010 17th IEEE International Conference on: IEEE; 2010. p. 4093-6.
33. Dice LR. Measures of the amount of ecologic association between species. Ecology 1945;26:297-302.